

Bulletin of the Seismological Society of America

This copy is for distribution only by
the authors of the article and their institutions
in accordance with the Open Access Policy of the
Seismological Society of America.

For more information see the publications section
of the SSA website at www.seismosoc.org



THE SEISMOLOGICAL SOCIETY OF AMERICA
400 Evelyn Ave., Suite 201
Albany, CA 94706-1375
(510) 525-5474; FAX (510) 525-7204
www.seismosoc.org

Structural Analysis of a Previously Unknown Active Fault That Triggered the 2013 M_w 5.8 Awajishima Earthquake, Southwest Japan

by Aiming Lin, Souichi Katayama, Gang Rao,* and Yasu'uchi Kubota

Abstract The M_w 5.8 Awajishima earthquake occurred on 13 April 2013 in southwest Awaji Island, ~25 km southwest of the epicenter of the 1996 M_w 6.8 Kobe earthquake, southwest Japan. Analyses of aerial photographs and 3D perspective images, field investigations, and structural analysis of fault rocks reveal that: (1) a previously undocumented fault, here called the Yamada fault, strikes northwest–southeast and dips southwest at 86° along a topographic lineament at the geological boundary between Mesozoic granitic rocks and the late Pliocene–Quaternary Osaka Group composed of interbedded sandstone and mudstone; (2) the main shear zone of the Yamada fault consists of a fault core with a < 10 cm wide zone of fault gouge (generally 1–5 cm), a fault breccia zone of < 100 cm wide, and a damage zone of 10–50 m wide, composed of cataclastic rocks and fractures; (3) foliations characterized by S-C fabrics that have developed in the shear zone indicate a dominantly thrust fault sense, consistent with that revealed by the focal mechanism; and (4) coseismic surface ruptures occurred locally along the main trace of the Yamada fault, consisting of numerous short fissures ranging in length from centimeters to several meters and concentrated in a zone < 5 m wide. Our findings show that the newly identified Yamada fault is an active fault and that it is probably the fault on which the 2013 M_w 5.8 Awajishima earthquake occurred. Therefore, it is necessary to construct a fault model to better understand the deformation characteristics of the seismogenic source fault and for reassessing the seismic hazards on the densely populated Awaji Island of southwest Japan.

Introduction

The 2011 magnitude (M_w) 9.0 Tohoku (Japan) earthquake generated a violent tsunami that caused extensive damage and more than 23,500 fatalities along the east-northeast coast of the island of Honshu, Japan. Seismic inversion results reveal that a maximum slip of up to ~50 m occurred along a 500 km long fault plane (e.g., Ide *et al.*, 2011; Sato *et al.*, 2011). Following this huge earthquake, several other large earthquakes of $M \geq 6$ occurred in Honshu Island, Japan, including the 11 March 2011 M_w 5.9 Shizuoka earthquake, the 11 April 2011 M_w 6.6 Fukushima earthquake, and the 13 April 2013 M_w 5.8 Awajishima earthquake (Japan Meteorological Agency, 2013). The 2013 M_w 5.8 Awajishima earthquake occurred in southwest Awaji Island, southwest Japan, at 05:33 (JST) on 13 April 2013, ~25 km southwest of the epicenter of the 1995 M_w 7.2 Kobe earthquake (Fig. 1a,b). Seismic inversion results show that the focal depth was ~15 km. The earthquake had a thrust-dominated mechanism on a fault striking north-northwest–south-southeast and dipping south-

west at $\sim 70^\circ$, with a compression axis oriented east–west (Fig. 1c). Aftershocks that occurred on 13 April 2013 also lie along the southwest-dipping fault plane (Fig. 1d; Japan Meteorological Agency, 2013; National Research Institute for Earth Science and Disaster Prevention, 2013). A maximum seismic intensity of 6 (on the Japanese seven-point seismic intensity scale) was observed at the epicenter of the earthquake in southwest Awaji Island (Japan Meteorological Agency, 2013). Geological data show no previously documented northwest–southeast to north-northwest–south-southeast-striking active faults in the epicentral area that could have been associated with the 2013 earthquake. Only a northeast–southwest-striking fault, the Senzan fault, has previously been reported in the area (Figs. 1b and 2a). Therefore, it was considered that this earthquake occurred on an unknown blind fault (Headquarters for Earthquake Research Promotion, see Data and Resources).

To gain a better understanding of the surface deformation and damage associated with the 2013 M_w 5.8 Awajishima earthquake and the geological structure in the area around the epicenter, our survey group traveled to this area

*Now at the Department of Earth Sciences, Zhejiang University, Hangzhou 310027.

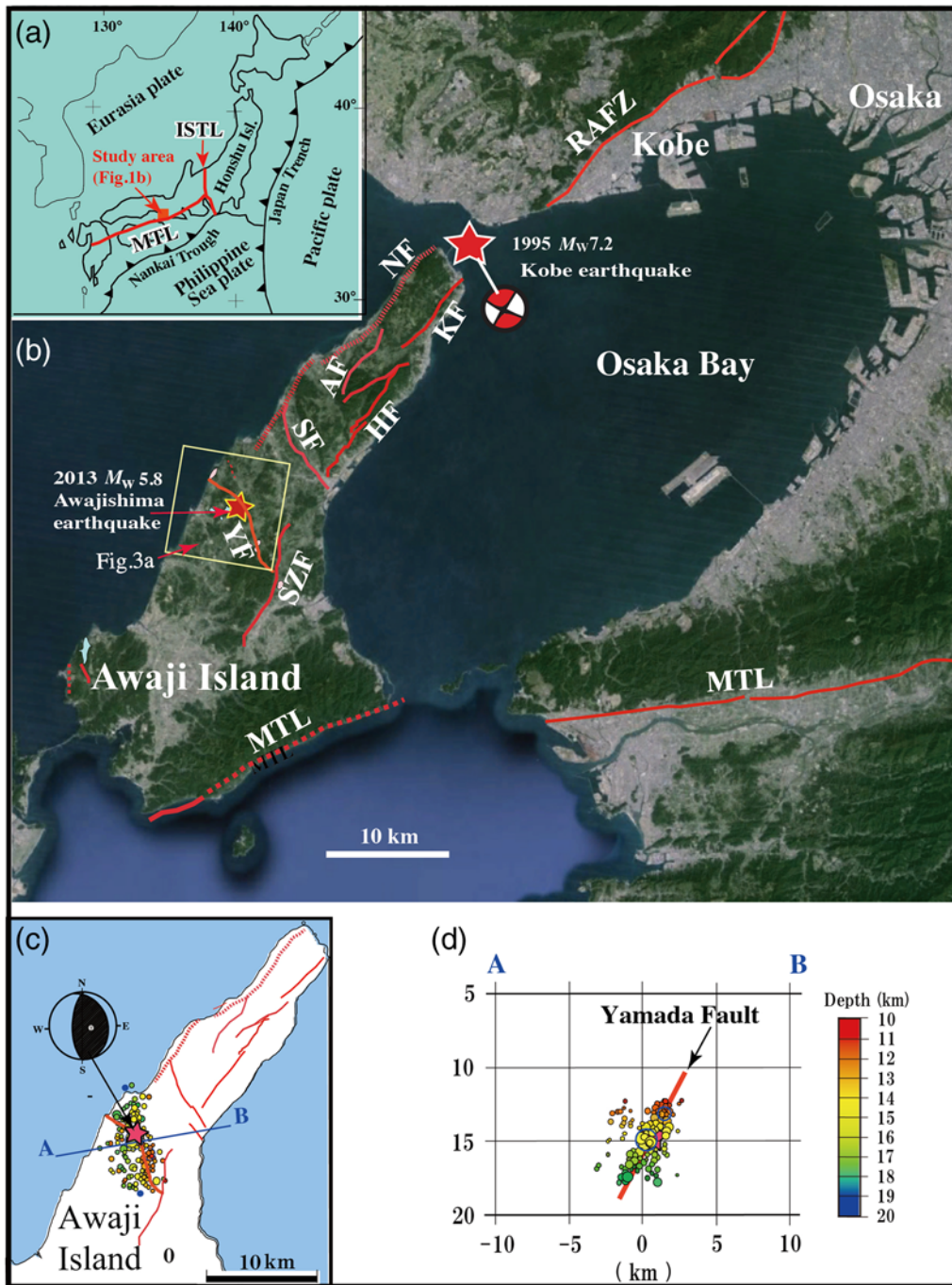


Figure 1. Index maps of the study area showing (a) the tectonic setting and (b) the distribution of active faults in the Awaji Island (Google image, active fault data are from [Research Group for Active Faults of Japan \[RGAFJ\], 1991](#)), and (c, d) the focal mechanism of the mainshock and the epicentral distribution of earthquakes that occurred on 13 April 2013 (data from the [Japan Meteorological Agency, 2013](#)). The Yamada fault (YF) is an active fault, newly reported in this study, on which it is believed that the 2013 Awajishima earthquake occurred. MTL, median tectonic line; ISTL, Itoigawa–Shizuoka tectonic line; RAFT, Arima-Takatsuki tectonic line; NF, Nojima fault; AF, Asano fault; KF, Kusumoto fault; SF, Shizuki fault; SZF, Senzan fault; Honshu Isl., Honshu Island. The color version of this figure is available only in the electronic edition.

the day after the earthquake. Primary data relating to the surface deformation caused by the earthquake were collected, and subsequent fieldwork was undertaken during the past year to investigate the fault structure. On the basis of the field investigations, we found a previously unmapped active fault, called Yamada fault (YF) here, that we believe is the fault on which

this earthquake occurred (Figs. 1 and 2a). This study focuses on the structural features of the newly found active fault and discusses the possibility that this is the fault on which the 2013 earthquake occurred. The implications of our findings for the seismotectonics of Awaji Island, southwest Japan, are also discussed.

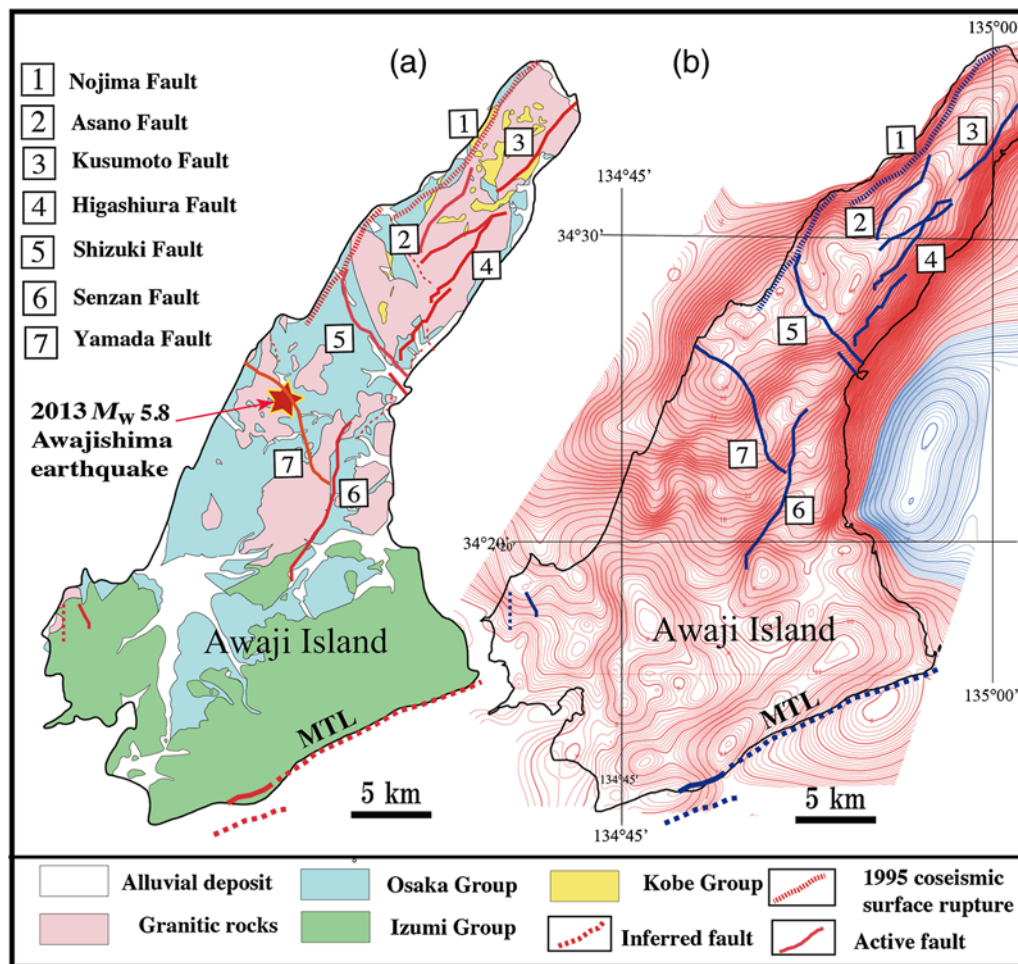


Figure 2. Maps showing (a) geology and (b) gravity anomaly of the Awaji Island. Geologic and gravity anomaly maps are modified from Takahashi *et al.* (1992) and Gravity Research Group in Japan (2001), respectively. The color version of this figure is available only in the electronic edition.

Tectonic Setting

The study area is located on the southwestern side of Awaji Island, in the marginal zone of the Eurasian plate and in the inner zone of southwest Japan (Fig. 1a). The median tectonic line (MTL), which is the longest tectonic lineament in Japan, runs along the southern coast of Awaji Island (Fig. 1b). The basement rocks consist mainly of Mesozoic granitic rocks and the Paleogene Kobe Group, unconformably overlain by the late Pliocene Osaka Group and Quaternary alluvial deposits (Fig. 2a; Takahashi *et al.*, 1992). The granitic host rocks are medium grained and consist mostly of quartz, feldspar, biotite, and minor amphibole. The Kobe Group occurs mainly in the northern-central area of Awaji Island, and the Osaka Group is widely distributed in the study area (Fig. 2a). The Kobe Group is composed mainly of sandstone, conglomerate, sandy mudstone, and thin intercalated lignite beds. The Osaka Group consists mainly of weakly consolidated sediments, including interbedded layers of mudstone, silt-sandstone, and conglomerate.

Several active faults are developed in this area. The Nojima, Asano, Kusumoto, Higashiura, and Senzan faults strike northeast–southwest. The Shizuki fault strikes northwest–southeast (Fig. 1b; Research Group for Active Faults of Japan [RGAFFJ], 1991), cutting the sediments of the Miocene–Pleistocene Kobe Group and Osaka Group and the Quaternary alluvial deposits. Approximately 18 km of surface ruptures associated with the 1995 M_w 7.2 Kobe earthquake occurred along the Nojima fault, accompanying coseismic right-lateral strike-slip movement of 1–2 m with a vertical slip component of < 1.5 m (Figs. 1b and 2a; Lin and Uda, 1996).

Contours of Bouguer gravity anomalies show a sharp change mostly along the boundary between the Mesozoic granitic rocks and the late Pliocene Osaka Group (Fig. 2). The contour lines change their trend from northwest–southeast in both the northwest and southeast segments to northeast–southwest in the central segment along the topographical lineament. The sudden change in the contour-line trend indicates the presence of a northwest–southeast-trend geologic boundary in the deep crust (Fig. 2b).

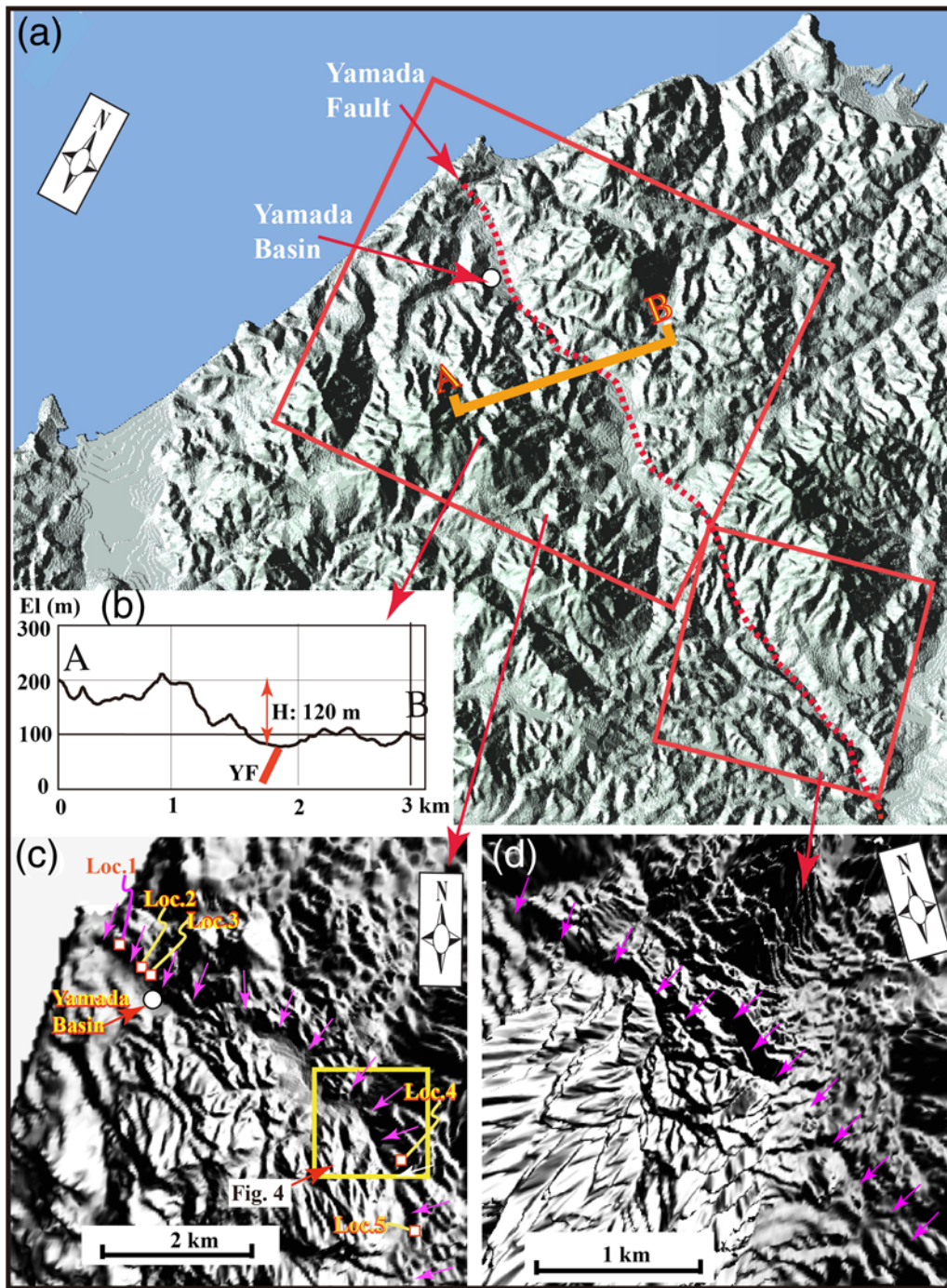


Figure 3. Gray-shaded relief maps showing the topographic features in the study area. (a) Perspective view of the linear landform. (b) Topographical profile across the YF. (c,d) Close up views of (a). Locations (Loc.) 1–5 are the main localities referred to in the text and in subsequent figures. Small arrows indicate the topographical lineament. The color version of this figure is available only in the electronic edition.

Topographic Features

To detect and identify tectonic-related topographic features in the study area, we examined aerial photographs, high-resolution Google Earth images, and color-shaded relief maps generated by 1/25,000 digital elevation model (DEM) data with a 10 m mesh grid, released by the Geospatial Infor-

mation Authority of Japan (see [Data and Resources](#)). To emphasize the visible fault scarps that strike northwest–southeast to north-northwest–south-southeast and face southwest or northeast, we illustrated the DEM from an azimuth of $N60^\circ W$ (Fig. 3a) and $N45^\circ E$ (Fig. 3c,d) at a sun angle of 10° above the horizon on the color-shaded relief maps. This made it possible to use a perspective view of images for identifying

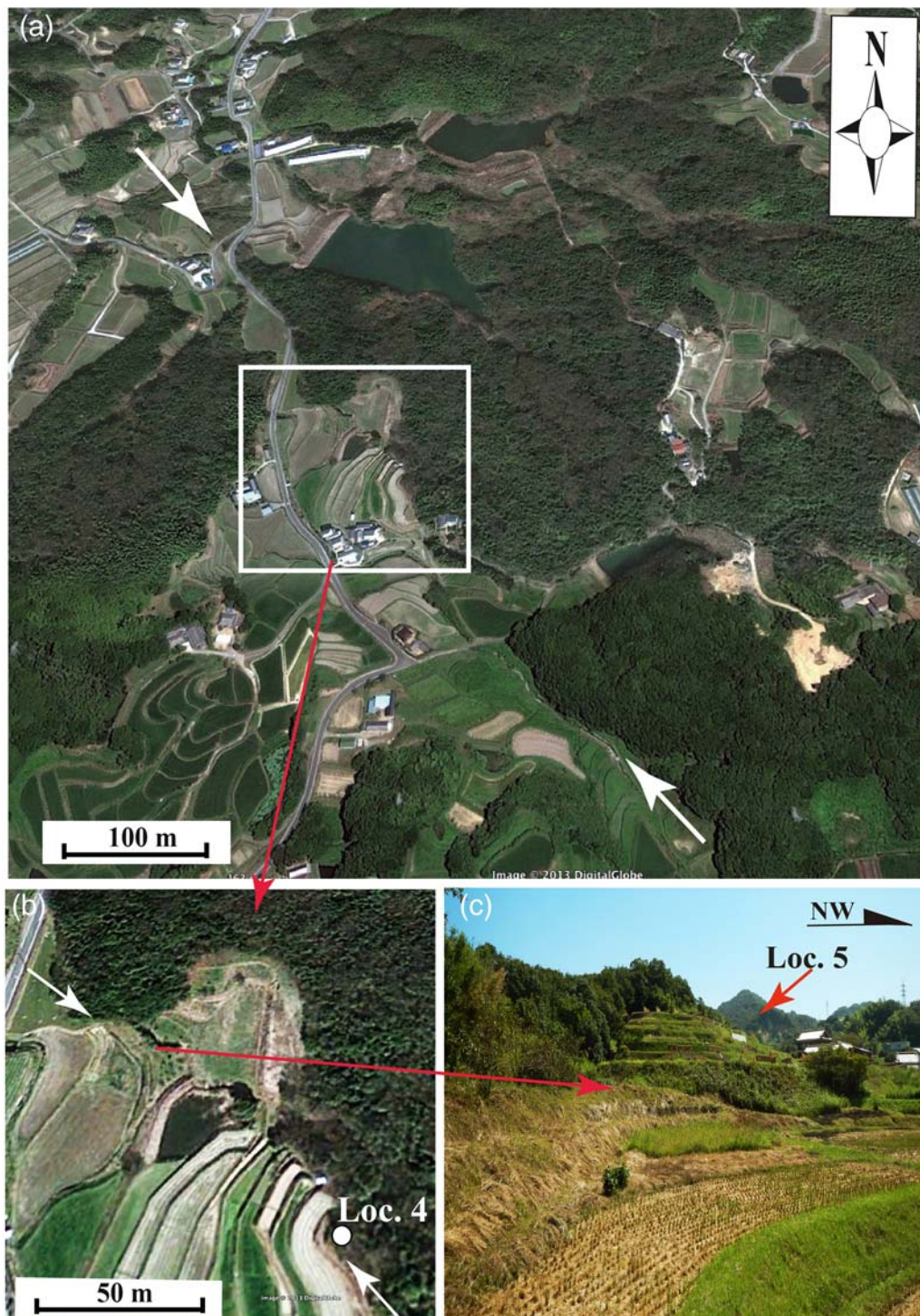


Figure 4. (a,b) Google Earth image showing the topographic lineament along a straight valley. (c) Field photograph showing the straight topographic feature shown in (b). The color version of this figure is available only in the electronic edition.

tectonic-related topographic features in vegetated areas. The tectonic-related topographic features identified by these methods were then confirmed in the field by excavating outcrops and observing the topographic features and fault zone structures.

On Awaji Island, most of the conspicuous topographic lineaments are developed along documented active faults

that are dominantly strike slip in nature (Fig. 1a; RGAFJ, 1991). In the epicentral area of the 2013 M_w 5.8 Awajishima earthquake, an ~ 10 km long northwest–southeast-striking topographic lineament can be recognized from the perspective topographic maps and the Google Earth images (Figs. 3 and 4a,b), which is mostly distributed along the geological boundary between granitic rocks and the late Pliocene Osaka

Group (Fig. 2a). However, it is not as conspicuous and straight as those developed along the well-known active faults on the island (Fig. 3a). In its northwestern segment, the lineament shows a curved shape along a northwest–southeast-trending narrow lowland (Yamada basin) and crosses through to another northwest–southeast-trending lowland in the southeast (Fig. 3a). A topographical profile shows that the southwestern side of the YF has been uplift for ~ 120 m (Fig. 3b). In the southeastern segment of the lineament, a distinct linear scarp is developed along a northwest–southeast linear valley (Figs. 3 and 4a,b), which is also validated by field investigations (Fig. 4c). The gravity anomaly map also shows a sharp change along this topographical lineament (Fig. 2b). These topographic features, geological structure, and gravity anomaly data indicate that the linear landform was probably formed mainly by faulting (see the Discussion section for details).

Structural Features of the Fault Zone

Fieldwork was guided by the perspective topographic maps and high-resolution Google Earth images. In the field, we found several fault outcrops and fault scarps along the topographic lineament and validated its tectonic origin. Based on the topographical features and fault zone structures described below, the newly found fault along the linear landform is called the YF in this study (Figs. 1b, 2–4).

To understand the ground deformation features associated with the 2013 earthquake and the relationship between the observed topographic lineament and the earthquake, we also excavated and cleaned a fault outcrop to make structural observations. Five typical fault outcrops at locations 1–5 along the YF (Fig. 3c) are described in detail below.

Location 1

At location (Loc.) 1, a fault outcrop is exposed along the geological boundary between granitic rocks and sandstones and mudstones of the Osaka Group, along the topographical lineament on a northeast-facing scarp with a dip angle of 20° – 30° (Fig. 5a). The main fault plane strikes $N35^\circ W$ and dips southwest at 80° . A fault shear zone of ~ 20 – 50 cm width is characterized by foliated cataclastic rocks and is observed to disrupt both the granitic rocks and the sediments of the Osaka Group (Fig. 5b,c). The foliation is generally parallel or subparallel to the main fault plane and is cut and offset by subfaults and fractures that are mostly filled by brownish soil material from the ground surface (Fig. 5d).

Location 2

A fault deformation zone of >10 m in width is found in a quarry within sediments of the Osaka Group, which consist mainly of interbedded mudstone and sandstone (Fig. 6). The sediment layers are deformed and tilted, dipping northeast at $\sim 30^\circ$ – 40° . Liquefaction structures such as irregular veins, dikes, and vein networks were injected along the fault plane and subsequently cut by faults and fractures (Fig. 6b–d). The

main faults cut and offset the sediment layers, liquefied dikes, and vein networks. The main fault planes strike northwest–southeast and dip southwest at $\sim 70^\circ$ – 80° . The structural features of the liquefied deposits indicate that liquefaction events were repeatedly induced by strong ground shaking during the period of deposition of the Osaka Group. These sediments were subsequently cut by faulting after the formation of the Osaka Group. Similar veins, dikes, and vein networks that formed in a submarine environment have been reported in the Nankai–Suruga trough to the south of Mt. Fuji and formed by repeated subduction zone earthquakes (Lin, 2006).

Location 3

At Loc. 3, the interbedded mudstone and sandstone layers of the Osaka Group are fault bounded along with alluvial deposits of sand–gravel, which are folded and tilted toward the scarp along the topographic lineament (Fig. 7a). A coseismic rupture zone of 5–20 cm wide was formed during the 2013 Awajishima earthquake along the fault, which was extended to the southeast through a vegetable field for more than 100 m in length (Fig. 7b). This rupture zone is composed of a series of short fractures showing a right-stepping en echelon pattern on a vertical exposure wall, indicating a northeast-down sense of movement, coincident with the topographic feature (Fig. 7b–d). Individual fractures range from ~ 10 to ~ 50 cm in length and < 3 cm in width. To understand the relationship between the coseismic surface ruptures and the fault itself, we excavated and cleaned the exposure (Fig. 7e). It is clear that the coseismic surface ruptures occurred only along the pre-existing fault shear zone in which the sediment layers have been disturbed and sheared (Fig. 7e). A fault shear zone of < 30 cm wide is observed, in which a thin fault gouge layer of ~ 2 – 5 cm wide, is developed along the main fault plane (Fig. 7e).

Location 4

At Loc. 4, the fault is exposed on a linear scarp developed along the topographical lineament (Fig. 8a). The fault scarp facing to the northeast with a dip angle of 45° is ~ 3 – 4 m in height. The interbedded layers of sandstone and conglomerate of the Osaka Group dip southwest at an angle of 30° and are offset by a fault striking northwest–southeast and dipping northeast at 80° (Fig. 8b). The deformation features of these strata indicate that the fault has been activated after the deposition of the Osaka Group during the late Pliocene. This topographical scarp extends to the southwest (to Loc. 5) over > 200 m, where the structural features of the fault zone are well observed.

Location 5

At Loc. 5, a fault outcrop was found in granitic rocks at a > 10 m high topographical scarp that extends from Loc. 4 (see Fig. 3c for locations) (Fig. 9a,b). The cataclasite derived from the granitic rocks is uplifted to the southwest and is a

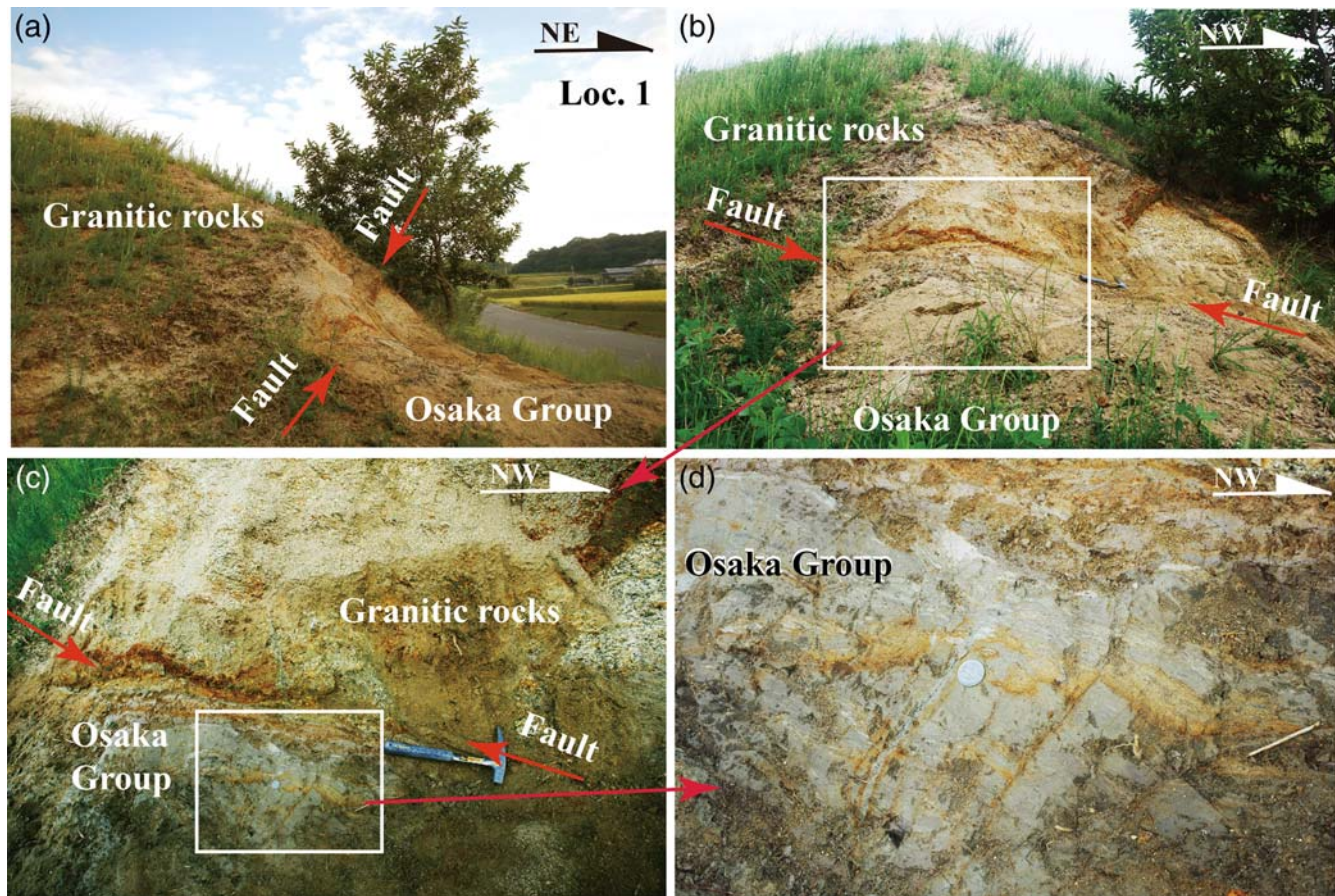


Figure 5. Representative field photographs showing the fault outcrop and coseismic fractures at Loc. 1. (a) Fault outcrop is exposed on a topographical scarp. (b) Fault outcrop developed along the boundary between granitic rocks and mudstone of the Osaka Group. (c) Close up view of (b). (d) Foliation developed in the mudstone is cut and offset by faults and fractures that are filled by soil material from the ground surface. The color version of this figure is available only in the electronic edition.

hard, cohesive rock (Fig. 9b). The fault core zone is ~50 cm to 2 m wide and is composed of fault breccia and fault gouge, in which foliation structures characterized by aggregates of fragments aligned parallel to the fault plane and discrete fractures are observed (Figs. 9c and 10). It is bounded by two main fault planes both striking northwest–southeast and dipping southwest and northwest, respectively, with dips of ~70°–80° (Figs. 9c and 10). A coseismic surface rupture zone of 10–20 cm wide occurs within the fault breccia zone, which extends for more than 10 m in length (Fig. 9c). Thin fault gouge zones (< 10 cm thick, generally 1–5 cm), which are incohesive and unconsolidated, are developed along the two main fault planes. A layered structure with at least three thin layers with different colors occurs in each gouge zone (Fig. 10). The fault breccia zone is bounded by layers of fault gouge on each side. The zone is composed of unconsolidated angular fragments ranging from submillimeter to 10 cm in size and a fine-grained matrix (Fig. 10a,b). Striations on the main fault plane indicate a thrust-dominated movement sense with a little right-lateral strike-slip component on the fault plane dipping northwest (Fig. 10a,c,e). Topographic features indicate that the southwestern side of the fault has been up-

lifted and the vertical striations indicate a thrust-dominant slip sense (Fig. 10a,c,e).

Microstructural Analysis of Fault Gouge

To observe and characterize the deformation microstructures within the fault shear zone at Loc. 5, we collected samples of fault rocks and cut the hand specimens along the sections parallel to the X–Z plane of the finite strain ellipsoid and then polished for structural analysis (Fig. 11).

The host granitic rocks show mosaic structures of quartz and feldspar crystals and are white gray in color with some microcracks observable under the stereomicroscope (Fig. 9a). In contrast, the cataclasite is characterized by numerous microcracks filled by fine-grained material (Fig. 11b). The fault breccia zone has an irregular boundary with the cataclasite, which is composed of angular fragments in a fine-grained matrix (Fig. 11b). The foliation observed in the fault gouge zones (Fig. 10b,c) is characterized by S–C fabrics (using the terminology of foliated cataclastic rocks of Lin, 1999, 2001, 2008) (Fig. 11c,d). The S planes are defined by the preferred orientation of rock/mineral fragments and fine-grained aggregates, similar in nature to those observed on the polished

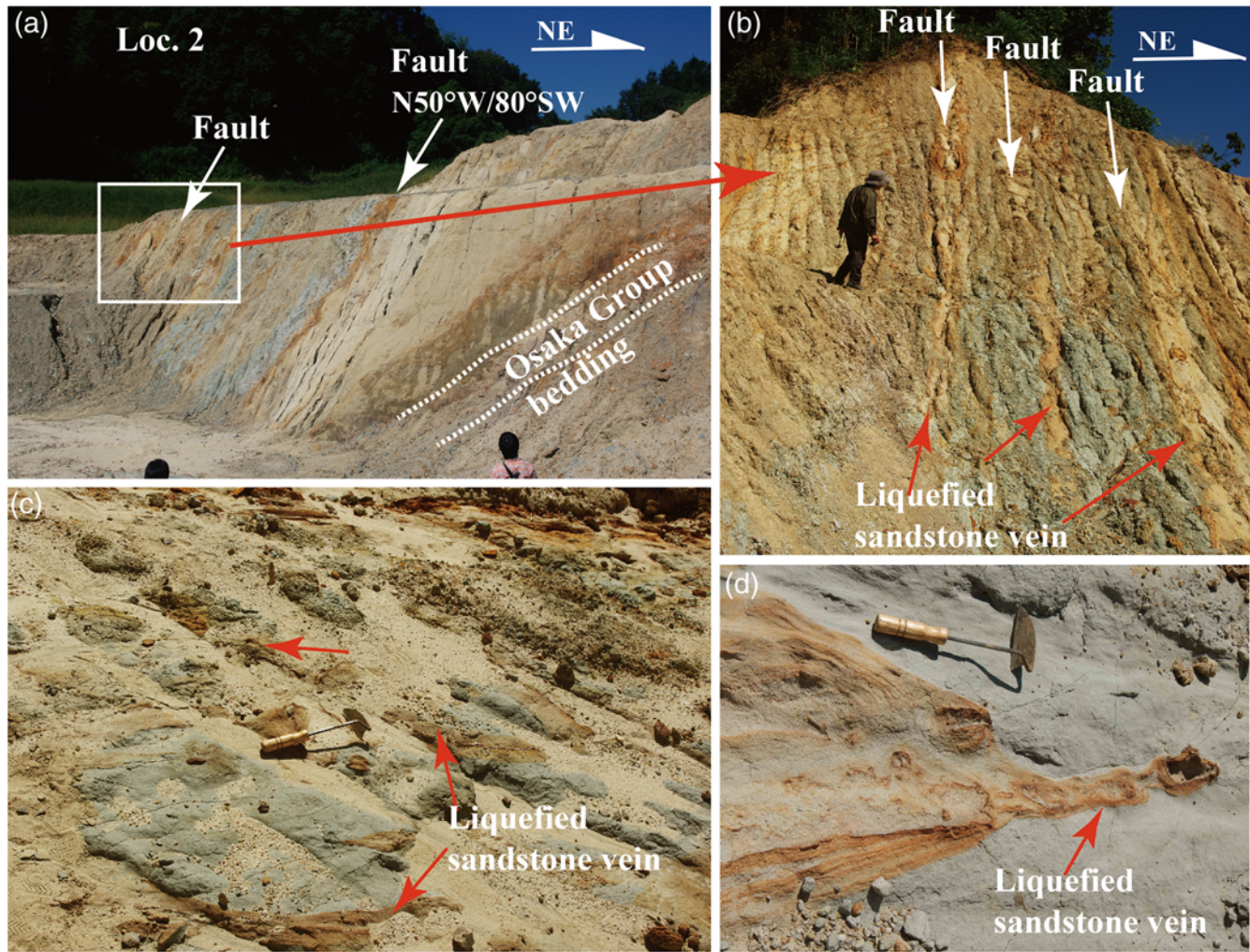


Figure 6. Representative field photographs of the fault outcrop at Loc. 2. (a) Overview of the fault outcrop developed in the Osaka Group. Note that the interbedded layers of mudstone and sandstone dip to the southwest at $\sim 30^\circ$. (b) Close up view of (a). Liquefied sand veins are injected along the fault zones. (c) Liquefied sandstone veins (indicated by arrows) are injected into the mudstone as simple lenses and complicated networks. (d) Liquefied sandstone veins in the mudstone. The color version of this figure is available only in the electronic edition.

sections of hand specimen observed in the field at Loc. 5 (Fig. 11). These aggregates of rock fragments and fine-grained material show a sigmoidal shape similar in form to the pressure shadow textures observed in mylonitic rocks (Fig. 11). The C and C' planes are defined mainly by microshear bands containing fine-grained material. The S-C fabrics observed in the incohesive fault gouge indicate southwest-up movement, consistent with that observed in the field (Figs. 10 and 11).

Discussion and Conclusions

Recent Activity of the Yamada Fault

Tectonic-related topographic features that develop around active faults and folds record displacements and ground deformation during large magnitude earthquakes. Studies of tectonic-related topography are essential for developing a historic and/or paleoseismic perspective of the locations, magnitudes, recurrence intervals, and slip patterns of seismogenic

faults (e.g., [RGAFJ, 1991](#); [Yeats et al., 1997](#); [Lin et al., 2009, 2013](#)). In another sense, structural features of fault zone and fault rocks provide primary evidence of the faulting history of crustal (structural) domains, as well as the deformation processes linked with seismic slip from the near surface to deep crust (e.g., [Sibson, 1977](#); [Lin et al., 2005](#); [Lin, 2008](#)). It is therefore possible to gain insights into the formation processes that operated throughout the history of faulting in a region, by studying the tectonic-related topographic features and characteristic structures of fault rocks exposed at the surface.

The northwest–southeast to north–northwest–south–southeast-trending topographical lineament identified in this study shows a curved and irregular approximately linear feature, differing from the lineaments developed along previously known strike-slip faults on Awaji Island, which are generally much straighter (Figs. 1b, 2a, and 3). The linear landform is developed in an intermontane area, so here there are no distinct surface deformation markers, such as terrace

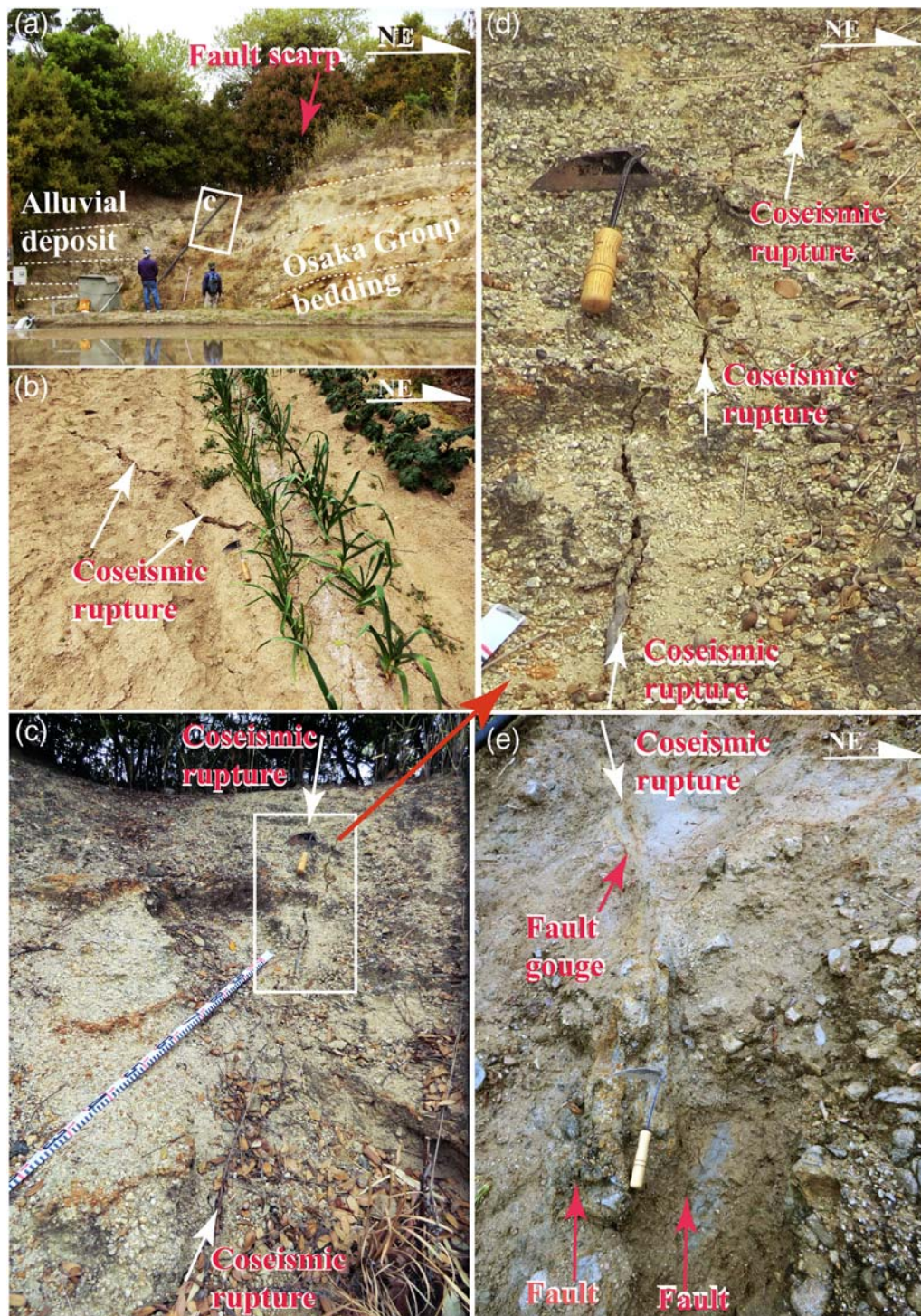


Figure 7. Representative field photographs of the fault outcrop at Loc. 3. (a) Overview of the fault outcrop at Loc. 3. Note that the sediment layers of the Osaka Group have been folded. (b) Coseismic surface ruptures in a vegetable field located ~100 m southwest of the fault outcrop at Loc. 3. (c) Coseismic surface ruptures at the boundary between the Osaka Group and unconsolidated alluvial deposits. (d) Close up view of the coseismic surface ruptures shown in (c). (e) Exposed fault zone along the coseismic surface rupture zone shown in (c). Note the coseismic surface rupture zone duplicated on the pre-existing fault zone. Thin fault gouge layer (2–3 cm wide) is developed along the fault plane. The color version of this figure is available only in the electronic edition.

risers and alluvial fans, which can be used to identify the recent activity of the fault. The irregular geometry and lack of surface deformation markers may be the main reasons that

the linear landform of the YF has not been considered as a tectonic-related lineament associated with an active fault in previous studies (e.g., [RGAFJ, 1991](#)). However, the structural

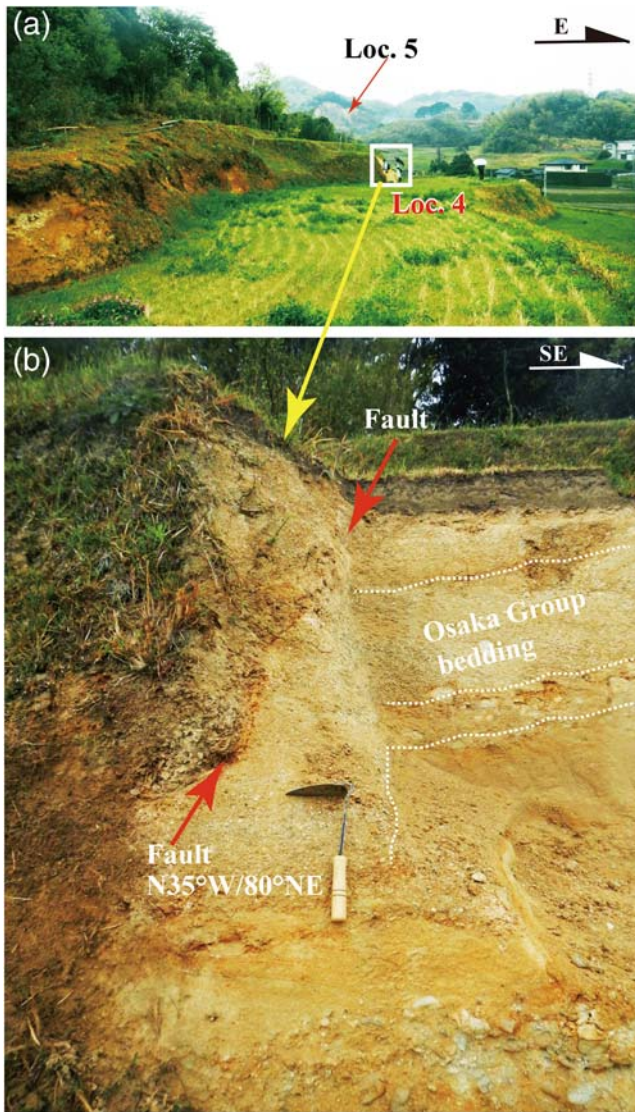


Figure 8. Representative field photographs of the fault outcrop at Loc. 4. (a) Overview of the outcrop. The fault outcrop is exposed on the edge of a topographical scarp. (b) The fault cuts sandstone and conglomerate layers of the Osaka Group. The color version of this figure is available only in the electronic edition.

features observed in the outcrops found in this study show that a fault exists along the linear landform and along the geological boundary between granitic rocks and the Osaka Group. The topographical profile shows a total vertical offset of >120 m with uplift of the southwestern side of the fault, indicating a displacement accumulated in the late Pliocene since the formation of the Osaka Group (Fig. 3b). The gravity anomaly data also reveal the presence of a geological boundary in deep crust (Fig. 2b). Furthermore, it would be difficult to form such a linear landform by erosion and degradation, along a northwest–southeast-trending narrow lowland and straight valley that also cuts across the mountain ranges through saddles for ~ 10 km (Fig. 3), by erosion and degradation. Generally, active thrust faults show irregular

traces within intermontane areas or along topographical boundaries between mountains and basins. These faults can be difficult to recognize from the nonlinear topographical features and irregular fault traces, for example, the thrust faults of the Longmen Shan Thrust Belt that triggered the 2008 M_w 7.9 Wenchuan earthquake (Lin *et al.*, 2009). The topographical features, fault zone structures, and gravity anomaly data indicate that the linear landform developed along the YF mainly by faulting.

As stated above, a variety of fault rocks are developed within the YF zone, including cohesive cataclasite and incohesive fault gouge and fault breccias. The 5–10 cm thick fault gouge layers with different colors developed along the main fault planes are shown by the interlayering of gray, yellowish-gray, and brownish-gray layers. The thickness and striped nature of the fault gouge is comparable with the gouge observed in fault outcrops and drilling cores of the Nojima fault, which triggered the 1996 M_w 7.2 Kobe, Japan, earthquake in northern Awaji Island (e.g., Shigetomi and Lin, 1999; Lin *et al.*, 2001). The layered structure developed in an ~ 5 –20 cm thick fault gouge of the Nojima fault is considered to be caused by multiple seismic faulting events (e.g., Shigetomi and Lin, 1999; Lin, 2001). Recent transmission electron microscope analyses revealed the presence of amorphous material in the fault gouge zone of the Nojima fault, which confirmed the idea that the layered fault gouge formed by seismic slip (Janssen *et al.*, 2013).

The accumulated evidence indicates that localization of coseismic shearing of a zone of <10 cm wide on planar faults is widespread throughout the crustal seismogenic zone, with extreme localization to less than 1 cm not uncommon (Sibson, 2003). Previous studies have shown that (1) seismic faulting in a fault zone occurs along prominent fracture surfaces that generally range from a few millimeters to a few centimeters in width (e.g., Chester and Chester, 1998; Lin, 2001); (2) coseismic slip during individual large earthquakes is localized in a narrow zone of <1 –3 mm within the fault gouge along the active fault trace; and (3) the individual color layers of the fault gouge may record at least one seismic slip event, for example, the Nojima fault during the 1995 Kobe M_w 6.8 earthquake (Shigetomi and Lin, 1999; Lin *et al.*, 2001), the Chelungpu fault during the 1999 Chi-Chi (Taiwan) M_w 7.6 earthquake (Heermance *et al.*, 2003; Lin *et al.*, 2005), the Longmen Shan Thrust Belt during the 2008 M_w 7.9 earthquake (Lin, 2011), and the Shionohira and Yunodake faults during the 2011 M_w 6.6 Fukushima (Japan) earthquake (Lin *et al.*, 2013). Experimental work has also demonstrated that seismic slip is concentrated in a zone of <1 mm wide (Mizoguchi *et al.*, 2007). Accordingly, we suggest that the ~ 5 –10 cm thick layered fault gouge records multiple seismic faulting events that have occurred on the YF.

It is also well known that incohesive cataclastic rocks, including fault gouge and fault breccia, form at shallow depths of <1 –4 km, assuming a geothermal gradient of $30^\circ\text{C}/\text{km}$ within the continental crust (Sibson, 1977; Lin, 2008). Accordingly, the cataclastic rocks including foliated

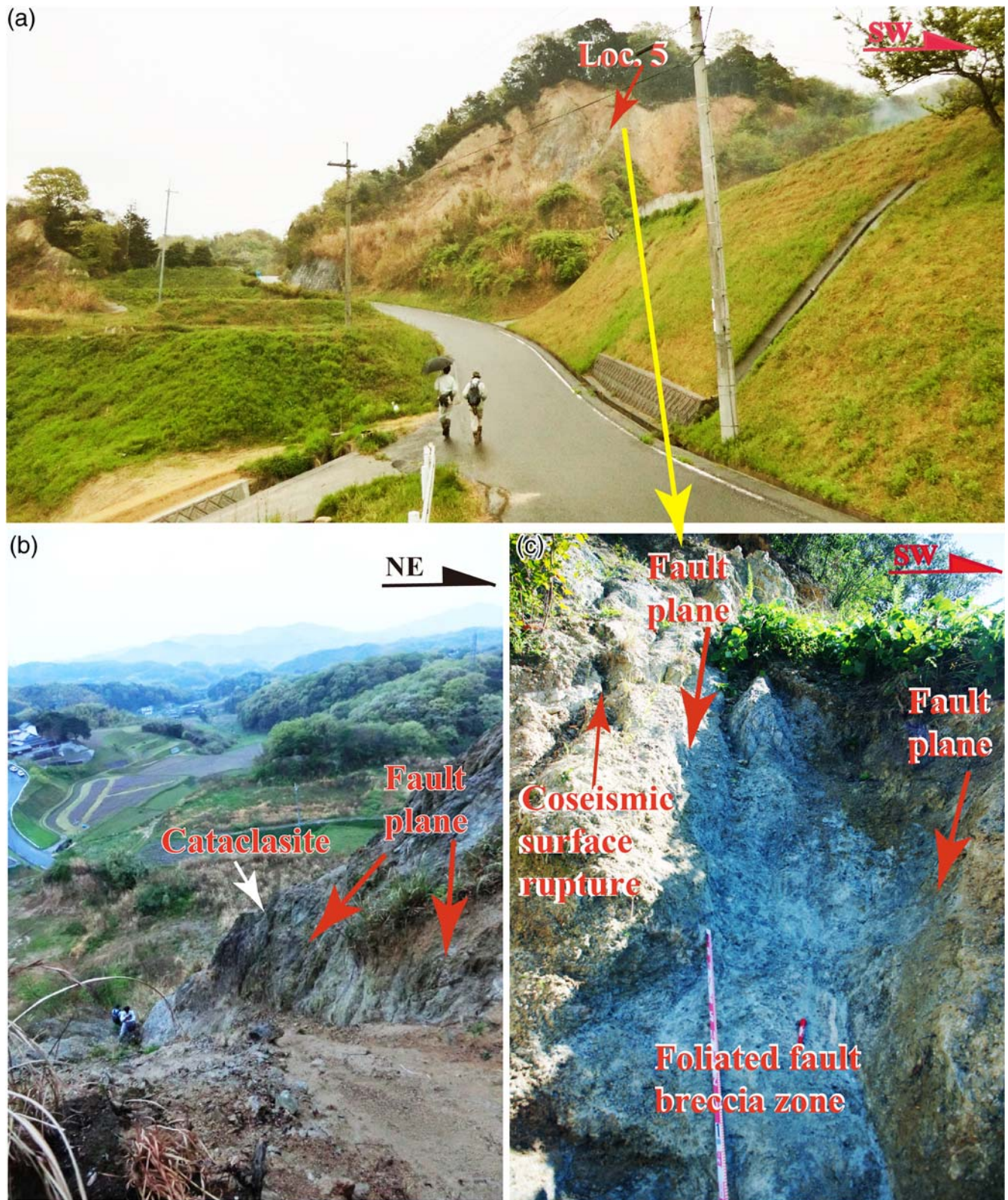


Figure 9. Representative field photographs of the fault outcrop at Loc. 5. (a) Overview of the outcrop. The fault outcrop is exposed on an ~10 m high topographical scarp. (b) Northwestward view of the linear landform from the outcrop at Loc. 5. (c) The fault breccia zone is bounded by two main fault planes. The color version of this figure is available only in the electronic edition.

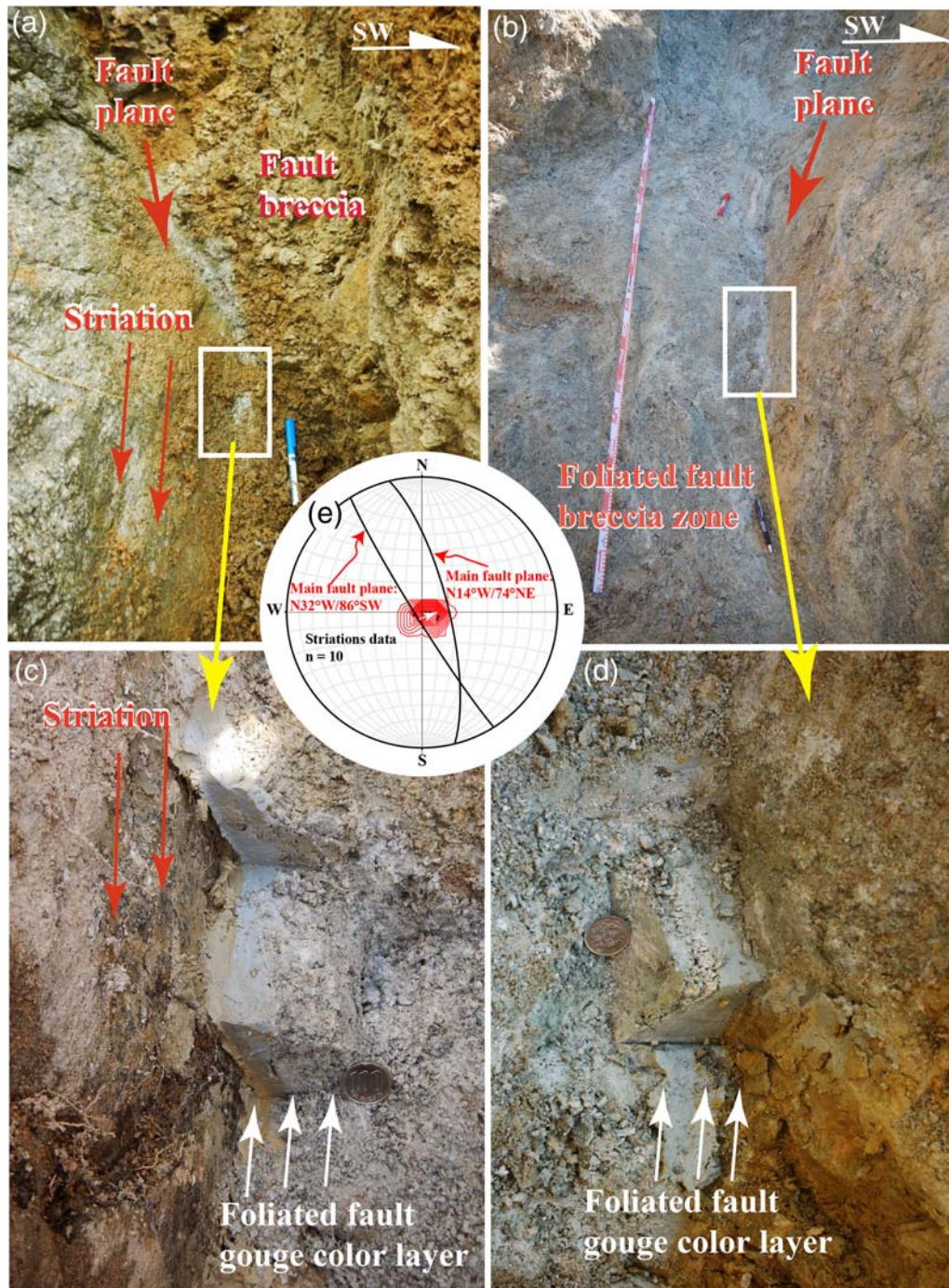


Figure 10. (a–d) Representative field photographs of the fault outcrop at Loc. 5 and (e) stereographic projection of striations. (a, b) Fault shear zone composed of fault breccia and fault gouge layers. Note that the striations developed on the fault plane plunge vertically. (c) Fault gouge layers bounded by a fault plane dipping northeast on which the striations are observed. (d) Fault gouge layers bounded by a fault plane dipping southwest. (e) Stereographic projection showing the orientations of striations on the main fault plane shown in (c). Arrow indicates the slip vector of hanging wall. Contour interval is 5% per 1% area. The color version of this figure is available only in the electronic edition.

fault gouge and fault breccia that developed along the YFs are inferred to have formed at relatively shallow depths of <4 km and to have been preserved in the fault zone and/or exhumed during subsequent episodes of uplift and erosion. The average present-day uplift and erosion rate is estimated to be 1–2 mm/yr in the southwest Japan (Yoshikawa *et al.*,

1981). Considering the present day rate of erosion and uplift and the formation depth of the fault gouge, we estimate that the fault gouge developed in the YF formed during the past 2–4 Ma. Geological evidence shows that the Osaka Group, within which the fault gouge layers occur in the study area, formed in the late Pliocene (~3.6 Ma) (Takahashi *et al.*,

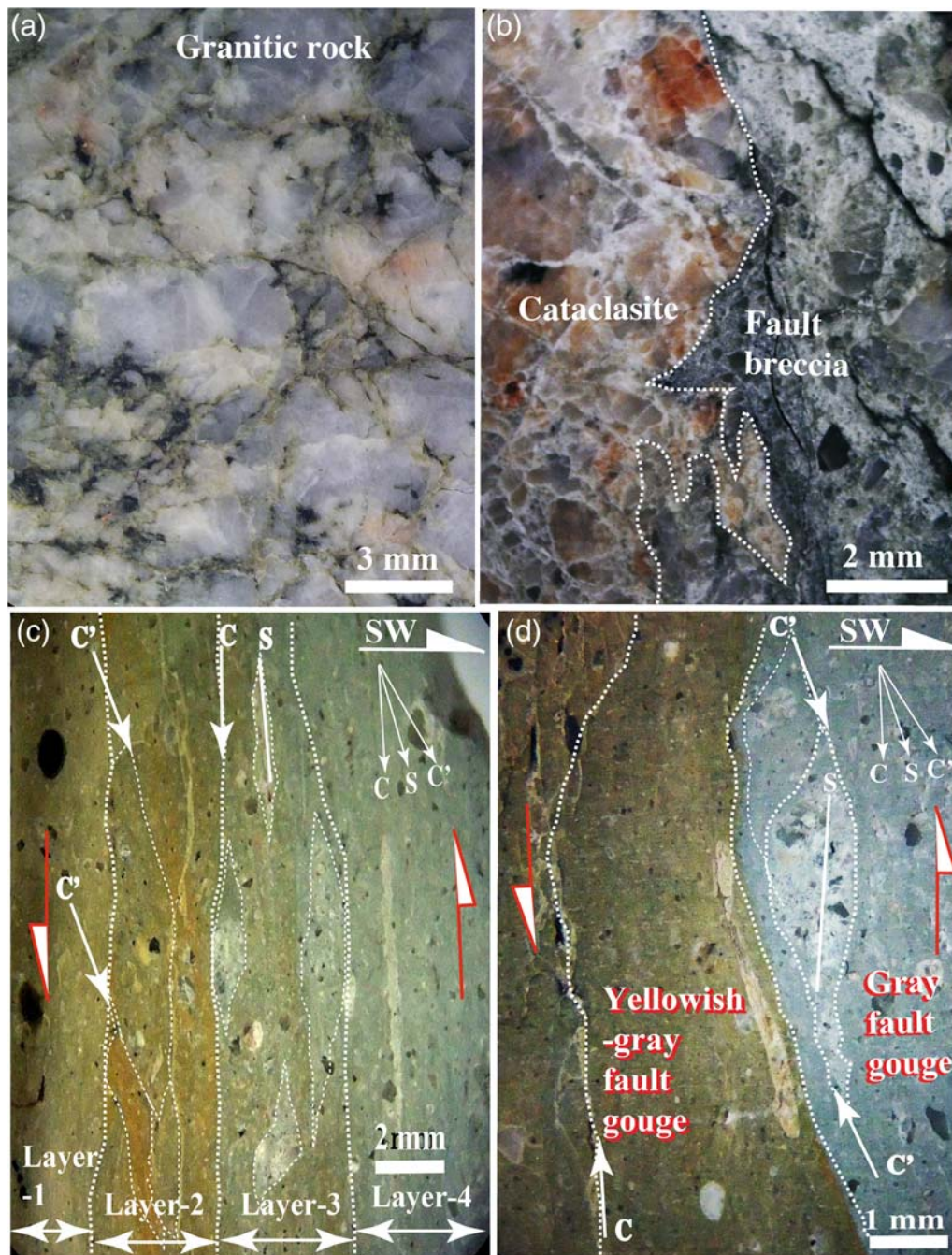


Figure 11. Photomicrographs showing the structural features of cataclastic rocks from Loc. 5. (a) Host granitic rocks with microcracks observed on a polished section under a stereomicroscope. (b) Cataclasite bounded by a fault breccia zone along an irregular boundary. (c,d) Fault gouge zone with layered structure characterized by S-C fabric. Layers 1–4 indicate the fault gouge layers with different colors. S-C and C' planar fabrics indicate southwest-up movement (half arrows). The color version of this figure is available only in the electronic edition.

1992), consistent with the above estimation of formation timing for the fault gouge. Therefore, the presence of an ~5–10 cm thick fault gouge zone indicates that seismic faulting events have occurred repeatedly within the YF since the formation of the Osaka Group, that is, during the past 2–3.6 Ma. Based on the relationship between lengths (L) of active faults and the earthquake magnitudes (M) ($\log L = 0.6M - 2.9$; Matsuda, 1975), the ~10 km long YF can therefore be regarded as an

active fault that has a potential to trigger a large earthquake of magnitude ~6.5.

In summary, the analytical results of topographical features and fault zone structures reveal that the topographic lineament developed along the geological boundary between Mesozoic granitic rocks and the late Pliocene–Quaternary Osaka Group is a newly found active fault that has been active as a seismogenic fault since the late Pliocene.

Relationship between the Yamada Fault and the Awajishima Earthquake

As most large earthquakes are caused by slip along active faults, any investigation of the seismic faulting process requires an understanding of the nature and geology of seismogenic fault zones (Lin *et al.*, 2013). Focal mechanisms suggest that the 2013 M_w 5.8 Awajishima earthquake occurred on a thrust fault striking north-northwest–south-southeast and dipping southwest at $\sim 70^\circ$ or dipping southeast at $< 30^\circ$ (Fig. 1c; Japan Meteorological Agency, 2013). Aftershocks are concentrated in a northwest–southeast-trending zone around the linear landform with a high dip angle of $\sim 70^\circ$ (Fig. 1d; National Research Institute for Earth Science and Disaster Prevention, 2013). As stated above, the S-C fabrics and striations developed on the main fault plane reveal a thrust-dominant movement sense with a little right-lateral strike-slip component and uplift of the southwestern side of the fault (Figs. 9 and 10). The field observations agree well with the fault plane inferred from the focal mechanism of the main earthquake and the distribution of aftershocks. Furthermore, accompanying this earthquake, coseismic surface ruptures composed of numerous short fissures ranging from centimeters to several meters in length and concentrated in a zone of < 5 m wide developed along the YF (Figs. 7 and 9c). These seismic data and structural features of the fault zone indicate that the YF is the fault that triggered the 2013 M_w 5.8 Awajishima.

During the past 20 years since the 1995 M_w 6.9 Kobe earthquake, many studies investigated the active faults in the Awaji Island (e.g., Lin and Uda, 1996; Lin, 2001; Murata *et al.*, 2001) and assessed the seismic hazard associated with the active faults in the Awaji Island (e.g., Headquarters for Earthquake Research Promotion, see Data and Resources), but the YF is not considered as a seismogenic fault that has a potential to trigger a large earthquake. Therefore, it is necessary to reconstruct the fault model for studying fault nature and recent activity including the slip rate and paleoseismicity and to reassess the seismic hazard of active faults for the densely populated Awaji Island, southwest Japan.

Data and Resources

Focal mechanisms and epicenters of the 2013 M_w 5.8 Awajishima earthquake were extracted from Japan Meteorological Agency (searched using www.jma.go.jp/jma/press/1304/13a/kaisetsu201304130730.pdf; last accessed January 2015). 1/25,000 digital elevation model data were downloaded from the Geospatial Information Authority of Japan (http://www.gsi.go.jp/ENGLISH/page_e30031.html; last accessed January 2015). Headquarters for Earthquake Research Promotion, Evaluation of Earthquake near Awajishima on 13 April 2013 is available at <http://www.jishin.go.jp/main/index-e.html> (last accessed March 2014).

Acknowledgments

We are grateful to B. Sherrod and an anonymous reviewer for critical reviews that helped to improve the manuscript. We thank K. Iida for help with processing the perspective maps, and to Y. Inoue and B. Yan for assistance in the field. This work was supported by a Science Project (Number 23253002) of the Ministry of Education, Culture, Sports, Science and Technology of Japan.

References

- Chester, F. M., and J. S. Chester (1998). Ultracataclastic structure and friction processes of the Punchbowl Fault, San Andreas system, California, *Tectonophysics* **295**, 199–221.
- Gravity Research Group in Japan (2001). Gravity Anomaly Map around Hanshin–Awaji Area, *Bulletin of the Nagoya University Museum Special Report No. 9*.
- Heermance, R., Z. K. Shipton, and J. P. Evans (2003). Fault structure control on fault slip and ground motion during the 1999 rupture of the Chelungpu fault, *Bull. Seismol. Soc. Am.* **93**, 1034–1050.
- Ide, S., A. Baltazy, and G. C. Beroza (2011). Shallow dynamic overshoot and energetic deep rupture in the 2011 M_w 9.0 Tohoku-Oki earthquake, *Science* **332**, 1426–1429.
- Janssen, C., R. Wirth, A. Lin, and G. Dresen (2013). TEM microstructural analysis in a fault gouge sample of the Nojima Fault Zone, Japan, *Tectonophysics* **583**, 101–104.
- Japan Meteorological Agency (2013). *The Earthquake near Awajishima at 5:33, April 13, 2013*, www.jma.go.jp/jma/press/1304/13a/kaisetsu201304130730.pdf (last accessed February 2014).
- Lin, A. (1999). S-C cataclastic in granitic rock, *Tectonophysics* **304**, 257–273.
- Lin, A. (2001). S-C fabrics developed in cataclastic rocks from the Nojima fault zone, Japan and their implications for tectonic history, *J. Struct. Geol.* **23**, 1167–1178.
- Lin, A. (2006). Repeated large subduction zone earthquakes in the Nankai-Suruga trough: Evidence from submarine liquefactions, *Geophys. Res. Lett.* **33**, L20314, doi: [10.1029/2006GL027952](https://doi.org/10.1029/2006GL027952).
- Lin, A. (2008). *Fossil Earthquakes: The Formation and Preservation of Pseudotachylites*, Springer-Verlag, Berlin, Heidelberg, Germany, 348 pp., ISBN: 978-3-540-74235-7.
- Lin, A. (2011). Seismic slip recorded in the fluidized ultracataclastic veins formed along the coseismic shear zone during the 2008 M_w 7.9 Wenchuan earthquake, *Geology* **39**, 547–550.
- Lin, A., and S. Uda (1996). Morphological characteristics of the earthquake surface ruptures occurred on Awaji Island, associated with the 1995 southern Hyogo Prefecture earthquake, *Island Arc* **5**, 1–15.
- Lin, A., C. Lee, T. Maruyama, and A. Chen (2005). Meso- and micro-structures of coseismic shear zone of the 1999 M_w 7.6 Chi-Chi earthquake, Taiwan, *Bull. Seismol. Soc. Am.* **95**, 486–501.
- Lin, A., Z. Ren, D. Jia, and X. Wu (2009). Co-seismic thrusting rupture and slip distribution produced by the 2008 M_w 7.9 Wenchuan earthquake, China, *Tectonophysics* **471**, 203–215.
- Lin, A., T. Shimamoto, T. Maruyama, M. Shigetomi, M. Takao, K. Takemura, H. Tanaka, S. Uda, and A. Murata (2001). Comparative study of the cataclastic rocks from a core and outcrops of the Nojima fault on Awaji Island, Japan, *Island Arc* **10**, 368–380.
- Lin, A., T. Shinji, G. Rao, S. Tsuchihashi, and B. Yan (2013). Structural analysis of coseismic normal fault zones of the M_w 6.6 Fukushima earthquake, northeast Japan, *Bull. Seismol. Soc. Am.* **103**, 1603–1613.
- Matsuda, T. (1975). Magnitude and recurrence interval of earthquake from a fault, *Zisin* **28**, 269–283 (in Japanese with English abstract).
- Mizoguchi, K., T. Hirose, T. Shimamoto, and E. Fukuyama (2007). Reconstruction of seismic faulting by high-velocity friction experiments: An example of the 1995 Kobe earthquake, *Geophys. Res. Lett.* **34**, L01308, doi: [10.1029/2006GL027931](https://doi.org/10.1029/2006GL027931).
- Murata, A., K. Takemura, T. Miyata, and A. Lin (2001). Vertical displacement and average slip rate of the Nojima fault, *Island Arc* **10**, 300–307.

- National Research Institute for Earth Science, and Disaster Prevention (2013). *13 April 2013 Awajishima Earthquake and Its Aftershock Distribution*, http://www.jishin.go.jp/main/chousa/13apr_awaji/p03.htm (last accessed March 2014).
- Research Group for Active Faults of Japan (RGAFJ) (1991). *Active Faults in Japan—Sheet Maps and Inventories* (revised edition), Univ. Tokyo Press, Tokyo, Japan, 437 pp. (in Japanese with English summary).
- Sato, M., T. Ishikawa, N. Ujihara, S. Yoshida, M. Fujita, M. Mochizuki, and A. Asada (2011). Displacement above the Hypocenter of the 2011 Tohoku-Oki earthquake, *Science* **332**, 1395.
- Shigetomi, M., and A. Lin (1999). Seismic events inferred from the layering structures of fault zones and pseudotachylytes in the Nojima fault zone, Japan, *Struct. Geol.* **43**, 33–42 (in Japanese with English abstract).
- Sibson, R. H. (1977). Fault rocks and fault mechanisms, *J. Geol. Soc. Lond.* **133**, 191–213.
- Sibson, R. H. (2003). Thickness of the seismic slip zone, *Bull. Seismol. Soc. Am.* **93**, 1169–1178.
- Takahashi, Y., A. Sangawa, K. Mizuno, and H. Hattori (1992). *Geology of the Sumoto District. Quadrangle Series*, Scale 1:50,000, 107 pp., Geological Survey of Japan.
- Yeats, R. S., K. Sieh, and C. R. Allen (1997). *The Geology of Earthquakes*, Oxford Univ. Press, Oxford, United Kingdom, 568 pp.
- Yoshikawa, T., S. Kaizuka, and Y. Ota (1981). *The Landforms of Japan*, University of Tokyo Press, Tokyo, Japan, 222 pp. (in Japanese).

Department of Geophysics
 Graduate School of Science
 Kyoto University
 Kyoto 606-8502, Japan
 slin@kugi.kyoto-u.ac.jp
 (A.L., S.K., G.R.)

OYO Cooperation
 Kobe 651-0083, Japan
 kubota-yasuuchi@oyonet.oyo.co.jp
 (Y.K.)

Manuscript received 2 May 2014;
 Published Online 21 April 2015